

Retrospective Cost Adaptive Control with Error-Dependent Regularization for MIMO Systems with Uncertain Nonminimum-Phase Transmission Zeros

E. Dogan Sumer*, Dennis S. Bernstein†

University of Michigan, Ann Arbor, Michigan, 48109-2140, USA

In this paper we focus on retrospective cost adaptive control (RCAC), which is applicable to stabilization, command following, disturbance rejection, and model reference control problems for SISO and MIMO plants. RCAC uses limited modeling information, specifically, Markov parameters of the transfer function from the control input to the performance variable. Typically, a small number of Markov parameters are needed, for example, one Markov parameter usually suffices if the plant is minimum phase. If the plant is Lyapunov stable and nonminimum phase, then knowledge of the locations of the nonminimum-phase zeros is not needed as long as an error-dependent regularization term is used to weight the control effort. For plants that are both open-loop unstable and nonminimum phase, knowledge of the locations of the nonminimum-phase zeros may be needed. The goal of the present paper is to further investigate the effectiveness of the error-dependent regularization terms. Furthermore, we remove the intermediate step of reconstructing the retrospective controls and we directly update the controller. Next, we consider channel-wise phase-matching conditions for MIMO plants. Finally, we investigate the role of zeros in MIMO nonsquare systems.

I. Introduction

In many applications of control, a model of the plant that is sufficiently accurate for controller synthesis is not available. A model with sufficient fidelity may be lacking due to either complex physics that are not amenable to first principles analysis or the inability to collect a sufficient amount of quality data for empirical modeling. Even if a sufficiently accurate model is available, the plant may undergo unexpected changes that cannot be accounted for prior to control-system operation. In some cases, the controller can be tuned iteratively online until desired performance is obtained. However, for safety-critical applications [1], the control system must be relied on to maintain performance despite these changes. These cases motivate the need for adaptive control, where the controller tunes itself to the actual plant during operation.

Although adaptive control reduces the need for plant modeling, it does not eliminate it completely. This modeling information may be obtained through either an offline identification process, leading to direct adaptive control, or a simultaneous identification process, leading to indirect adaptive control. In either case, it stands to reason that the less modeling information that an adaptive controller needs, the more robust it is to model uncertainty. This observation evokes the following question: What modeling information is essential for an adaptive controller to control a plant to a specified level of performance? Our objective is to minimize this modeling information without limiting the class of plants to which adaptive control can be applied.

In this paper we focus on retrospective cost adaptive control (RCAC), which is applicable to stabilization, command following, disturbance rejection, and model reference control problems for SISO and MIMO plants [2–4, 6]. RCAC uses limited modeling information, specifically, Markov parameters of the transfer function from the control input to the performance variable. Typically, a small number of Markov parameters are needed, for example, one Markov parameter usually suffices if the plant is minimum phase. If the plant is asymptotically stable and nonminimum phase, then knowledge of the locations of the nonminimum-phase zeros is not needed as long as an error-dependent regularization term is used to weight the control effort [7].

*Graduate Student, Department of Aerospace Engineering, AIAA Student Member

†Professor, Department of Aerospace Engineering, AIAA Member.

For plants that are both open-loop unstable and nonminimum phase, knowledge of the locations of the nonminimum-phase zeros may be needed. Robustness of RCAC to knowledge of the Markov parameters is investigated in [8], where it is shown that a phase-matching property is a sufficient condition for adaptively controlling open-loop asymptotically stable nonminimum-phase systems with unknown nonminimum-phase zeros. This phase matching condition can be met by system identification methods independently of Markov parameter estimation.

The goal of the present paper is to further investigate the effectiveness of the error-dependent regularization used in [7]. Unlike [7], we remove the intermediate step of reconstructing the retrospective controls and, as in [4], we directly update the controller. We do this for an instantaneous cost function as in [4] as well as for a cumulative cost function as in [6]. In addition, and unlike [4], we modify the cost function by filtering the data used in the regularization term.

In Section II we describe the RCAC algorithm. We then proceed to investigate two specific issues. First we consider phase-matching conditions within a MIMO context. We do this numerically in order to determine whether channel-wise phase matching is sufficient to ensure stable operation of the algorithm. Finally, we investigate the role of zeros in MISO and SIMO systems. In this case, we show that nonminimum-phase direction zeros [9,10] are crucial to the performance of the adaptive controller.

II. Retrospective Cost Adaptive Control

A. Problem Formulation

Consider the MIMO discrete-time system

$$x(k+1) = Ax(k) + Bu(k) + D_1w(k), \quad (1)$$

$$y(k) = Cx(k) + D_2w(k), \quad (2)$$

$$z(k) = E_1x(k) + E_0w(k), \quad (3)$$

where $x(k) \in \mathbb{R}^n$, $y(k) \in \mathbb{R}^{l_y}$, $z(k) \in \mathbb{R}^{l_z}$, $u(k) \in \mathbb{R}^{l_u}$, $w(k) \in \mathbb{R}^{l_w}$, and $k \geq 0$. The system (1)–(3) can represent a sampled-data application arising from a continuous-time system with sample and hold operations.

We represent (1), (3) as the time-series model

$$z(k) = \sum_{i=1}^n -\alpha_i z(k-i) + \sum_{i=d}^n \beta_i u(k-i) + \sum_{i=0}^n \gamma_i w(k-i), \quad (4)$$

where d is the smallest integer such that β_d is not zero. The plant (1),(3) is represented by the operator matrices

$$G_{zu}(\mathbf{q}) \triangleq E_1(\mathbf{q}I - A)^{-1}B, \quad (5)$$

$$G_{zw}(\mathbf{q}) \triangleq E_1(\mathbf{q}I - A)^{-1}D_1 + E_0, \quad (6)$$

where \mathbf{q} is the forward shift operator and, unlike the z -transform, (5),(6) accounts for possibly nonzero initial conditions. Furthermore, for each positive integer i ,

$$H_i \triangleq E_1 A^{i-1} B$$

is the i^{th} Markov parameter of G_{zu} .

Now, consider the n_c^{th} -order strictly proper output feedback controller

$$x_c(k+1) = A_c(k)x_c(k) + B_c(k)y(k), \quad (7)$$

$$u(k) = C_c(k)x_c(k), \quad (8)$$

where $x_c \in \mathbb{R}^{n_c}$. The feedback control (7),(8) is represented by $u = G_c(\mathbf{q})y$, where

$$G_c(\mathbf{q}, k) \triangleq C_c(k)(\mathbf{q}I - A_c(k))^{-1}B_c(k). \quad (9)$$

The goal is to develop an adaptive output feedback controller to minimize the performance variable z in the presence of the exogenous signal w with limited modeling information about the dynamics and exogenous signal. We assume that the measurements $y(k)$ and $z(k)$ are available for feedback.

For the adaptive controller, the matrices $A_c(k)$, $B_c(k)$ and $C_c(k)$ may be time-dependent, and thus the transfer function model (9) illustrates the structure of the time-varying controller in which $A_c = A_c(k)$, $B_c = B_c(k)$, and $C_c = C_c(k)$.

B. Control Law

We use a linear, strictly proper time-series controller of order n_c such that the control $u(k)$ is given by

$$u(k) = \theta^T(k)\phi(k-1), \quad (10)$$

where

$$\theta(k) = \begin{bmatrix} N_1^T(k) & \cdots & N_{n_c}^T(k) & M_1^T(k) & \cdots & M_{n_c}^T(k) \end{bmatrix}^T \in \mathbb{R}^{n_c(l_u+l_y) \times l_u}, \quad (11)$$

$$\phi(k-1) = \begin{bmatrix} y^T(k-1) & \cdots & y^T(k-n_c) & u^T(k-1) & \cdots & u^T(k-n_c) \end{bmatrix}^T \in \mathbb{R}^{n_c(l_u+l_y)}. \quad (12)$$

The control law (10) can be reformulated as

$$u(k) = \Phi(k-1)\Theta(k), \quad (13)$$

where

$$\Phi(k-1) \triangleq I_{l_u} \otimes \phi^T(k-1) \in \mathbb{R}^{l_u \times l_u n_c(l_u+l_y)}, \quad (14)$$

$$\Theta(k) \triangleq \text{vec}(\theta(k)) \in \mathbb{R}^{l_u n_c(l_u+l_y)}, \quad (15)$$

“ \otimes ” denotes the Kronecker product, and “ vec ” is the column-stacking operator.

C. Retrospective Performance

For a positive integer r , we define

$$G_f(\mathbf{q}^{-1}) \triangleq K_1 \mathbf{q}^{-1} + K_2 \mathbf{q}^{-2} + \cdots + K_r \mathbf{q}^{-r}, \quad (16)$$

where $K_i \in \mathbb{R}^{l_z \times l_u}$ for $1 \leq i \leq r$. Next, for $k \geq 1$, we define the *retrospective performance variable*

$$\hat{z}(\hat{\Theta}(k), k) \triangleq z(k) + \Phi_f(k-1)\hat{\Theta}(k) - u_f(k) \in \mathbb{R}^{l_z}, \quad (17)$$

where

$$\Phi_f(k-1) \triangleq G_f(\mathbf{q}^{-1})\Phi(k-1) \in \mathbb{R}^{l_z \times l_u n_c(l_u+l_y)}, \quad (18)$$

$$u_f(k) \triangleq G_f(\mathbf{q}^{-1})u(k) \in \mathbb{R}^{l_z}, \quad (19)$$

for $k \leq 0$, $u(k) = 0$, $\Phi(k-1) = 0$, and, for $k \geq 1$, $\hat{\Theta}(k) \in \mathbb{R}^{l_u n_c(l_u+l_y)}$ is an optimization variable. The retrospective performance variable (17) can be rewritten in the form

$$\hat{z}(\hat{\Theta}(k), k) = z(k) + K_{zu} \left(\begin{bmatrix} \Phi(k-2) \\ \vdots \\ \Phi(k-r-1) \end{bmatrix} \hat{\Theta}(k) - \begin{bmatrix} u(k-1) \\ \vdots \\ u(k-r) \end{bmatrix} \right), \quad (20)$$

where $K_{zu} \triangleq \begin{bmatrix} K_1 & \cdots & K_r \end{bmatrix} \in \mathbb{R}^{l_z \times r l_u}$. The choice of K_{zu} is discussed in Sections IV and V.

D. Instantaneous Cost and Update Law

For $k \geq 0$, we define the instantaneous cost function

$$J_{\text{ins}}(\hat{\Theta}(k), k) \triangleq \hat{z}^T(\hat{\Theta}(k), k)R_1(k)\hat{z}(\hat{\Theta}(k), k) + \eta(k)\hat{\Theta}(k)^T\Phi_f^T(k-1)R_2(k)\Phi_f(k-1)\hat{\Theta}(k) \\ + \alpha(k)(\hat{\Theta}(k) - \Theta(k-1))^T R_3(k)(\hat{\Theta}(k) - \Theta(k-1)), \quad (21)$$

where, for all $k > 0$, $\alpha(k) > 0$ and $\eta(k) \geq 0$ are scalars, $R_1(k) \in \mathbb{R}^{l_z \times l_z}$ is positive definite, $R_2(k) \in \mathbb{R}^{l_z \times l_z}$ is positive semidefinite, and $R_3(k) \in \mathbb{R}^{l_u n_c(l_u + l_y) \times l_u n_c(l_u + l_y)}$ is positive definite. The control weighting $\eta(k)$ is chosen to be

$$\eta(k) = \eta_0 \sum_{i=0}^{p_c-1} z^T(k-i)z(k-i), \quad (22)$$

where $\eta_0 \geq 0$ and p_c is a positive integer. Now, substituting (17) into (21) yields

$$J_{\text{ins}}(\hat{\Theta}(k), k) = \hat{\Theta}(k)^T \Gamma_1(k) \hat{\Theta}(k) + \Gamma_2^T(k) \hat{\Theta}(k) + \Gamma_3(k), \quad (23)$$

where

$$\Gamma_1(k) \triangleq \Phi_f^T(k-1) [R_1(k) + \eta(k)R_2(k)] \Phi_f(k-1) + \alpha(k)R_3(k) \in \mathbb{R}^{l_u n_c(l_u + l_y) \times l_u n_c(l_u + l_y)}, \quad (24)$$

$$\Gamma_2(k) \triangleq 2\Phi_f^T(k-1)R_1(k) [z(k) - u_f(k)] - 2\alpha(k)R_3(k)\Theta(k-1) \in \mathbb{R}^{l_u n_c(l_u + l_y)}. \quad (25)$$

Since $\Gamma_1(k)$ is positive definite, $J_{\text{ins}}(\hat{\Theta}(k), k)$ has the unique global minimizer $\hat{\Theta}^*(k)$ for all $k \geq 0$, which yields the instantaneous update law

$$\Theta(k+1) = \hat{\Theta}^*(k) = -\frac{1}{2}\Gamma_1^{-1}(k)\Gamma_2(k). \quad (26)$$

E. Cumulative Cost and Update Law

For $k > 0$, we define the cumulative cost function

$$J_{\text{cum}}(\hat{\Theta}(k), k) \triangleq \sum_{i=1}^k \lambda^{k-i} (\hat{z}^T(\hat{\Theta}(k), i)R_1(i)\hat{z}(\hat{\Theta}(k), i) + \eta(i)\hat{\Theta}(k)^T\Phi_f^T(i-1)R_2(i)\Phi_f(i-1)\hat{\Theta}(k)) \\ + \lambda^k (\hat{\Theta}(k) - \Theta(0))^T P_0^{-1} (\hat{\Theta}(k) - \Theta(0)), \quad (27)$$

where $\lambda \in (0, 1]$, and $P_0 \in \mathbb{R}^{l_u n_c(l_u + l_y) \times l_u n_c(l_u + l_y)}$ is positive definite. Substituting (17) into (27) yields

$$J_{\text{cum}}(\hat{\Theta}(k), k) = \hat{\Theta}^T(k)\mathcal{A}(k)\hat{\Theta}(k) + \mathcal{B}^T(k)\hat{\Theta}(k) + \mathcal{C}(k), \quad (28)$$

where $\mathcal{A}(0) = P_0^{-1}$, $\mathcal{B}(0) = -2P_0^{-1}\Theta(0)$, and, for all $k \geq 1$,

$$\mathcal{A}(k) \triangleq \sum_{i=1}^k \lambda^{k-i} \Phi_f^T(i-1) [R_1(i) + \eta(i)R_2(i)] \Phi_f(i-1) + \lambda^k P_0^{-1}, \quad (29)$$

$$\mathcal{B}(k) \triangleq \sum_{i=1}^k 2\lambda^{k-i} \Phi_f^T(i-1)R_1(i) [z(i) - u_f(i)] - 2\lambda^k P_0^{-1}\Theta(0). \quad (30)$$

Since $\mathcal{A}(k)$ is positive definite, the cumulative cost function (27) has the unique global minimizer $\hat{\Theta}^*(k)$ for all $k \geq 0$, which yields the cumulative update law

$$\Theta(k+1) = \hat{\Theta}^*(k) = -\frac{1}{2}\mathcal{A}^{-1}(k)\mathcal{B}(k). \quad (31)$$

To reduce memory usage, $\mathcal{A}(k)$ and $\mathcal{B}(k)$ can be computed recursively using

$$\mathcal{A}(k) = \lambda\mathcal{A}(k-1) + \Phi_f^T(k-1) [R_1(k) + \eta(k)R_2(k)] \Phi_f(k-1), \quad (32)$$

$$\mathcal{B}(k) = \lambda\mathcal{B}(k-1) + 2\Phi_f^T(k-1)R_1(k) [z(k) - u_f(k)]. \quad (33)$$

Furthermore, (31) involves inversion of a matrix of size $l_u n_c(l_u + l_y) \times l_u n_c(l_u + l_y)$. The following lemma provides an alternative recursive computation that requires inversion of a matrix of size $l_z \times l_z$.

Proposition II.1. Let $R_1(k) \equiv R_2(k) \equiv I_{l_z}$, and, for $k \geq 1$, define $P(k) \triangleq \mathcal{A}^{-1}(k)$, where $P(0) = P_0 \in \mathbb{R}^{l_u n_c(l_u+l_y) \times l_u n_c(l_u+l_y)}$ is positive definite. Then, for all $k \geq 1$, $P(k)$ satisfies

$$P(k) = \frac{1}{\lambda} [P(k-1) - P(k-1)\Phi_f^T(k-1)\Lambda^{-1}(k)\Phi_f(k-1)P(k-1)], \quad (34)$$

where

$$\Lambda(k) \triangleq \frac{\lambda}{1+\eta(k)} I_{l_z} + \Phi_f(k-1)P(k-1)\Phi_f^T(k-1). \quad (35)$$

Furthermore, the cumulative cost function (27) has the unique global minimizer

$$\Theta(k+1) = \Theta(k) - \frac{1}{1+\eta(k)} P(k-1)\Phi_f^T(k-1)\Lambda^{-1}(k)\epsilon(k), \quad (36)$$

where

$$\epsilon(k) \triangleq z(k) - u_f(k) + (1+\eta(k))\hat{u}_f(k), \quad (37)$$

and

$$\hat{u}_f(k) \triangleq \Phi_f(k-1)\Theta(k). \quad (38)$$

Proof. From (32),

$$P^{-1}(k) = \lambda P^{-1}(k-1) + (1+\eta(k))\Phi_f^T(k-1)\Phi_f(k-1). \quad (39)$$

Applying the matrix inversion lemma to (39) yields

$$P(k) = \frac{1}{\lambda} P(k-1) \quad (40)$$

$$- \frac{1}{\lambda} P(k-1)\Phi_f^T(k-1) \left[\frac{\lambda}{1+\eta(k)} I_{l_z} + \Phi_f(k-1)P(k-1)\Phi_f^T(k-1) \right]^{-1} \Phi_f(k-1)P(k-1) \quad (41)$$

$$= \frac{1}{\lambda} [P(k-1) - P(k-1)\Phi_f^T(k-1)\Lambda^{-1}(k)\Phi_f(k-1)P(k-1)]. \quad (42)$$

Hence, (34) holds. Next, since $P(k) = \mathcal{A}^{-1}(k)$, it follows from (31), (33) and (34) that

$$\begin{aligned} \Theta(k+1) &= -\frac{1}{2}P(k)\mathcal{B}^T(k) \\ &= -\frac{1}{2}P(k-1)\mathcal{B}^T(k-1) - \frac{1}{\lambda}P(k-1)\Phi_f^T(k-1)[z(k) - u_f(k)] \\ &\quad + \frac{1}{2}P(k-1)\Phi_f^T(k-1)\Lambda^{-1}(k)\Phi_f(k-1)P(k-1)\mathcal{B}^T(k-1) \\ &\quad + \frac{1}{\lambda}P(k-1)\Phi_f^T(k-1)\Lambda^{-1}(k)\Phi_f(k-1)P(k-1)\Phi_f^T(k-1)[z(k) - u_f(k)] \\ &= \Theta(k) - \frac{1}{\lambda}P(k-1)\Phi_f^T(k-1)\Lambda^{-1}(k)\Lambda(k)[z(k) - u_f(k)] - P(k-1)\Phi_f^T(k-1)\Lambda^{-1}(k)\hat{u}_f(k) \\ &\quad + \frac{1}{\lambda}P(k-1)\Phi_f^T(k-1)\Lambda^{-1}(k)\Phi_f(k-1)P(k-1)\Phi_f^T(k-1)[z(k) - u_f(k)] \\ &= \Theta(k) - P(k-1)\Phi_f^T(k-1)\Lambda^{-1}(k) \\ &\quad \cdot \left(\hat{u}_f(k) + \left(\frac{1}{1+\eta(k)} I_{l_z} + \frac{1}{\lambda} \Phi_f(k-1)P(k-1)\Phi_f^T(k-1) - \frac{1}{\lambda} \Phi_f(k-1)P(k-1)\Phi_f^T(k-1) \right) [z(k) - u_f(k)] \right) \\ &= \Theta(k) - \frac{1}{1+\eta(k)} P(k-1)\Phi_f^T(k-1)\Lambda^{-1}(k)\epsilon(k). \quad \square \end{aligned}$$

III. Phase Matching Condition

Let $G_{zu,ij}$ denote the transfer function from the j^{th} input u_j to the i^{th} output z_i . Furthermore, let $G_{f,ij}$ denote the ij^{th} entry of G_f . Then, for $\theta \in [0, \pi]$, the *phase mismatch* $\Delta_{ij}(\theta)$ between $G_{f,ij}$ and $G_{zu,ij}$ is defined as

$$\Delta_{ij}(\theta) \triangleq \cos^{-1} \frac{\operatorname{Re} \left[G_{zu,ij}(e^{j\theta}) \overline{G_{f,ij}(e^{j\theta})} \right]}{|G_{zu,ij}(e^{j\theta})| |G_{f,ij}(e^{j\theta})|} \in [0, 180] \text{deg}. \quad (43)$$

Note that $\Delta_{ij}(\theta)$ represents the angle between $G_{zu,ij}(e^{j\theta})$ and $G_{f,ij}(e^{j\theta})$ in the complex plane. The role of phase mismatch in closed-loop performance of RCAC for SISO plants is investigated in [8]. Furthermore, frequency domain methods are presented for approximating IIR plants with FIR transfer functions in [12], although the use of A_{zu} provides greater flexibility for phase matching by allowing G_f to be an IIR transfer matrix.

IV. K_{zu} for SISO Plants

Techniques for constructing K_{zu} for SISO plants are discussed in [4, 11]. In [3], it is shown that the choice $K_{zu} = \begin{bmatrix} 0_{1 \times (d-1)} & H_d \end{bmatrix}$ provides asymptotic convergence of z to zero if the open-loop plant is minimum-phase. For nonminimum-phase plants, these methods construct K_{zu} such that the NMP zeros of G_f approximate the NMP zeros of G_{zu} .

In this section, we present a phase-matching-based technique for constructing K_{zu} . This technique is used for Lyapunov-stable, nonminimum-phase plants, and does not require knowledge of the nonminimum-phase zeros of the system. In Section V, we extend this technique to MIMO systems.

For unstable, nonminimum-phase plants, knowledge of the nonminimum-phase zero locations may be necessary. In this case, we use the NMP-zero-based methods presented in [4, 11].

A. Phase-matching-based Construction of K_{zu} for Lyapunov-Stable Plants with Unknown NMP zeros

For Lyapunov stable plants with unknown NMP zeros, we construct K_{zu} so that $\Delta(\theta) \leq 90$ deg for $\theta \in [0, \pi]$ rad/sample. This requires an estimate of the frequency response of $G_{zu}(e^{j\theta})$ for $\theta \in [0, \pi]$ rad/sample. To construct K_{zu} , we use the linear or the nonlinear fitting method outlined in [12].

If A is asymptotically stable, and the exogenous signal w is harmonic, it suffices to construct K_{zu} such that $\Delta(\theta) \leq 90$ deg at the exogenous signal frequencies. This requires an estimate of the frequency response of $G_{zu}(e^{j\theta})$ at each exogenous signal frequency.

V. K_{zu} for MIMO Plants

In [4, 11], construction of K_{zu} for MIMO plants uses Markov parameters H_i or time-series-coefficients β_i . For square systems, [3] shows that the choice $K_{zu} = \begin{bmatrix} 0_{l_z \times (d-1)l_u} & H_d \end{bmatrix}$ provides asymptotic convergence of z to zero if the transmission zeros of the open-loop plant are all minimum-phase and H_d is nonsingular. For MIMO plants with nonminimum-phase transmission zeros, these methods require that the transmission zeros of G_f approximate the transmission zeros of G_{zu} .

We now extend the phase-matching-based construction of K_{zu} for MIMO plants. As in the SISO case, the method does not apply to unstable plants with nonminimum-phase transmission zeros.

A. Channel-wise Phase-matching Based Construction of K_{zu} for Lyapunov Stable MIMO Plants with Unknown NMP Zeros

For Lyapunov-stable MIMO plants with unknown NMP transmission zeros, we extend the SISO method outlined in the previous section. In particular, we construct K_{zu} such that, for all $i \leq l_z$, $j \leq l_u$, $\Delta_{ij}(\theta) < 90$ deg for $\theta \in [0, \pi]$ rad/sample, and K_{zu} has full-row-rank. This requires an estimate of the frequency response of each input-output channel $G_{zu,ij}(e^{j\theta})$ for $\theta \in [0, \pi]$ rad/sample.

As in the SISO case, if the plant is asymptotically stable and the exogenous signal is harmonic, it suffices to construct K_{zu} such that, for all $i \leq l_z$, $j \leq l_u$, $\Delta_{ij}(\theta) < 90$ deg at each exogenous signal frequency, and K_{zu} has full-row-rank. This requires an estimate of the frequency response of each input-output channel $G_{zu,ij}(e^{j\theta})$ at each exogenous signal frequency.

VI. Numerical Examples

In this section, we present SISO and MIMO numerical examples illustrating RCAC. Except for the first example, we use the cumulative cost with the recursive equations (34)–(36) with $\lambda = 1$. In all examples, we assume that the performance variable z is the only measurement to be used in feedback, therefore, $y = z$. Furthermore, in all cases, we initialize the controller gain vector $\Theta(0)$ and the controller states $x_c(0)$ to be zero.

Example VI.1 (SISO, NMP, asymptotically stable plant, disturbance rejection with the instantaneous algorithm). Consider the SISO, lightly damped nonminimum-phase plant shown in Figure 1(a) with $n = 4$, $d = 1$, $H_1 = 1$, poles $0.95e^{\pm j\pi/5}$, $0.9e^{\pm j\pi/3}$, minimum-phase zero -0.2 , and nonminimum-phase zeros 1.25 , 2 . We consider the matched sinusoidal disturbance $w(k) = \sin \Theta_1 k$, where $\Theta_1 = 2\pi/5$ rad/sample. We let

$$K_{zu} = \begin{bmatrix} 1 & 0.308 & -0.586 & -0.165 & 0.768 & 0.726 \end{bmatrix}, \quad (44)$$

so that $\Delta(\theta) < 90$ for all $\theta \in [0, \pi]$ rad/sample. Note that the zeros of G_f do not approximate the NMP zeros of G_{zu} . Taking $n_c = 10$, $\eta_0 = 0.05$, $p_c = 1$, and $\alpha(k) \equiv 5000$, the closed-loop response is shown in Figure 1(b).

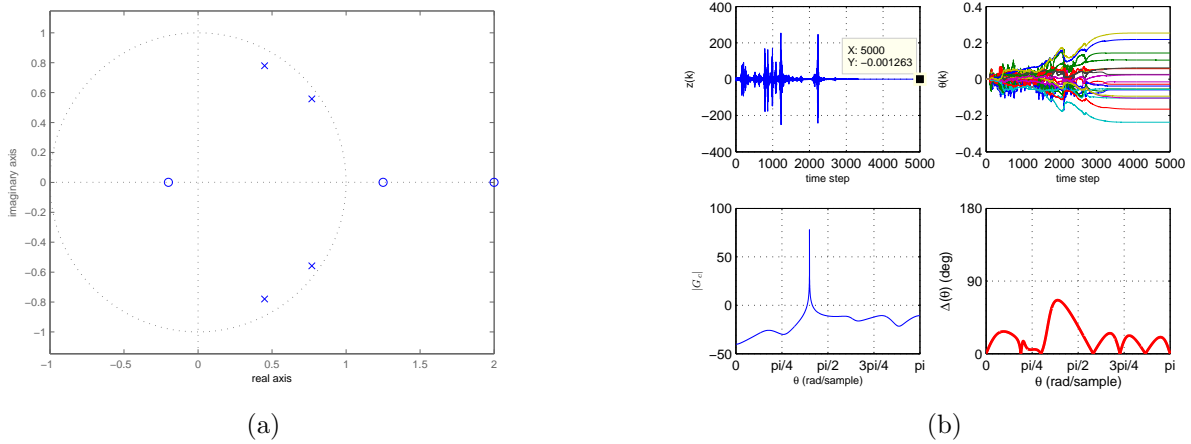


Figure 1. Example VI.1: SISO, asymptotically stable, nonminimum-phase plant. (a) shows the poles and zeros of G_{zu} , while (b) shows the closed-loop response. With the tuning parameters $n_c = 10$, $\eta_0 = 0.05$, $p_c = 1$ and $\alpha(k) \equiv 5000$, instantaneous RCAC is turned on at $k = 100$. After transients, the performance variable converges to zero, and RCAC converges to an internal model controller with high gain at the disturbance frequency $\Theta_1 = 2\pi/5$ rad/sample. Phase-matching-based construction of K_{zu} is used to satisfy $\Delta(\theta) < 90$ for all $\theta \in [0, \pi]$.

If $\eta_0 = 0$, the algorithm becomes the same as the instantaneous RCAC described in [4]. In this case, the zeros of G_f must include the NMP zeros of G_{zu} . We now consider the same matched disturbance, but take $\eta_0 = 0$, and take $K_{zu} = [H_1 \dots H_6]$. G_f now has the zeros 2.09 and 1.09 , which approximate the NMP zeros of G_{zu} . Taking $n_c = 10$ and $\alpha(k) \equiv 5000$, the closed-loop response is shown in Figure 2. ■

Example VI.2 (SISO, NMP, asymptotically stable plant, disturbance rejection with the cumulative algorithm). Consider the same plant considered in Example VI.1. We now consider the two-tone unmatched disturbance $w(k) = \begin{bmatrix} \sin \Theta_1 k & 1.5 \sin \Theta_2 k \end{bmatrix}$, where $\Theta_1 = 2\pi/5$ rad/sample and $\Theta_2 = 2\pi/3$ rad/sample.

With the plant realized in controllable canonical form, that is, $B = \begin{bmatrix} 1 & 0 & 0 & 0 \end{bmatrix}^T$, we take $D_1 = \begin{bmatrix} I_2 & 0_{2 \times 2} \end{bmatrix}^T$, so that the disturbance is not matched with the input.

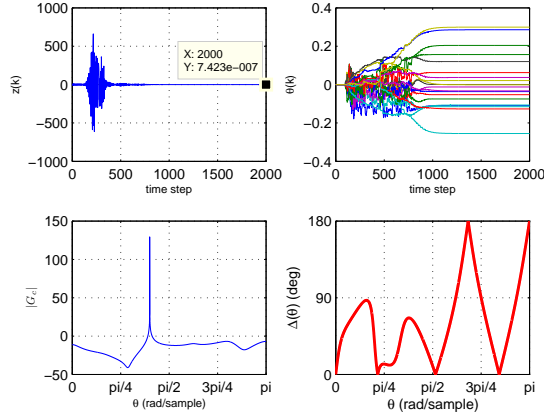


Figure 2. Example VI.1: SISO, asymptotically stable, nonminimum-phase plant, with Markov-parameter-based K_{zu} construction. Six Markov parameters are used in the construction, and the zeros of G_f approximate the nonminimum-phase zeros of G_{zu} . With the tuning parameters $n_c = 10$, $\eta_0 = 0.0$, and $\alpha(k) \equiv 5000$, instantaneous RCAC is turned on at $k = 100$. After transients, the performance variable converges to zero, and RCAC converges to an internal model controller with high-gain at the disturbance frequency $\theta = 2\pi/5$ rad/sample.

We first use the phase-matching-based approach by using error-dependent weighting $\eta(k)$ and taking K_{zu} as in (44) so that $\Delta(\theta) < 90$ deg for $\theta \in [0, \pi]$ rad/sample. Taking $n_c = 10$, $\eta_0 = 0.1$, $p_c = 1$, and $P_0 = 0.01I$, the closed-loop response is shown in Figure 3(a). Note the significant improvement in the transient performance compared to the response with the instantaneous update.

As discussed in Section IV, since the plant is asymptotically stable and the exogenous signal is harmonic, an alternative is to construct K_{zu} such that $\Delta(\theta) \leq 90$ deg at only the exogenous signal frequencies. This reduces the number of coefficients needed in the construction of K_{zu} . For instance, with $K_{zu} = H_1$, it follows that $\Delta(\Theta_1) < 90$ deg and $\Delta(\Theta_2) < 90$ deg as shown in Figure 3(b). Hence, taking $n_c = 10$, $\eta_0 = 0.1$, $p_c = 1$, and $P_0 = 0.01I$, the performance variable converges to zero as shown in Figure 3(b).

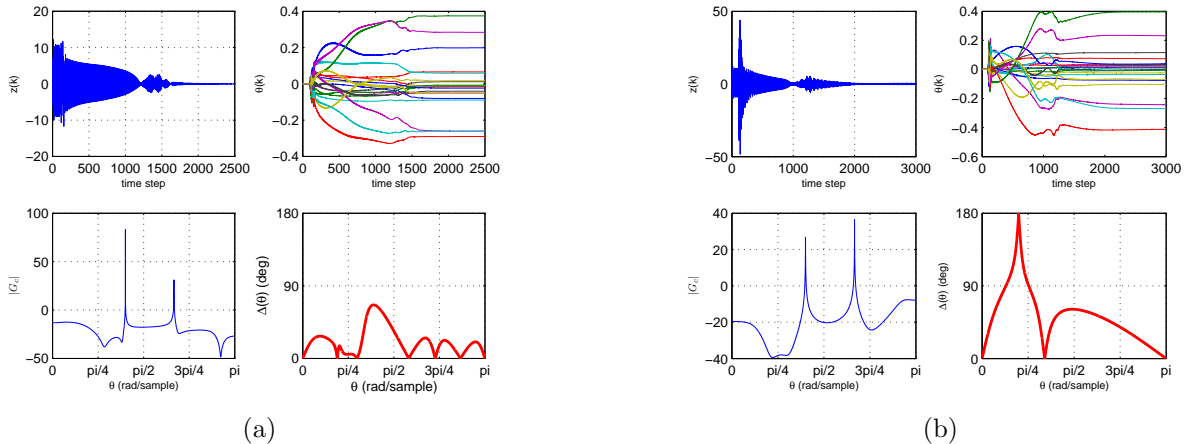


Figure 3. Example VI.2: SISO, NMP, asymptotically stable plant with the cumulative update law. (a) shows the closed-loop response when K_{zu} is constructed to have $\Delta(\theta) < 90$ for all $\theta \in [0, \pi]$, while (b) shows the closed-loop response with $K_{zu} = H_1$, which provides $\Delta(\theta) < 90$ for the exogenous frequencies $\Theta_1 = 2\pi/5$ rad/sample and $\Theta_2 = 2\pi/3$ rad/sample, but not for all θ . Same tuning parameters $n_c = 10$, $\eta_0 = 0.1$, $p_c = 0.1$ and $P_0 = 0.01I$ are used in both cases. The performance variable converges to zero in both cases, but (a) has superior transient performance compared to (b).

We now modify the algorithm and remove the performance-dependence property of the control weighting $\eta(k)$ by letting $\eta(k)$ be constant. We choose K_{zu} as given in (IV), and let $n_c = 10$, $p_c = 1$, $P_0 = 0.01I$. Taking $\eta(k) \equiv 5$ leads to destabilization of the closed-loop system as shown in Figure 4(a). Increasing the weighting to have $\eta(k) \equiv 10$ prevents destabilization, but the performance variable does not converge to

zero as shown 4(b). Similar results are obtained if a different constant weighting η is used, that is, either the closed-loop system is destabilized, or the performance variable does not converge to zero. These results stress the importance of the performance-dependence property of the control weighting term $\eta(k)$ when K_{zu} does not capture the NMP zeros of G_{zu} .

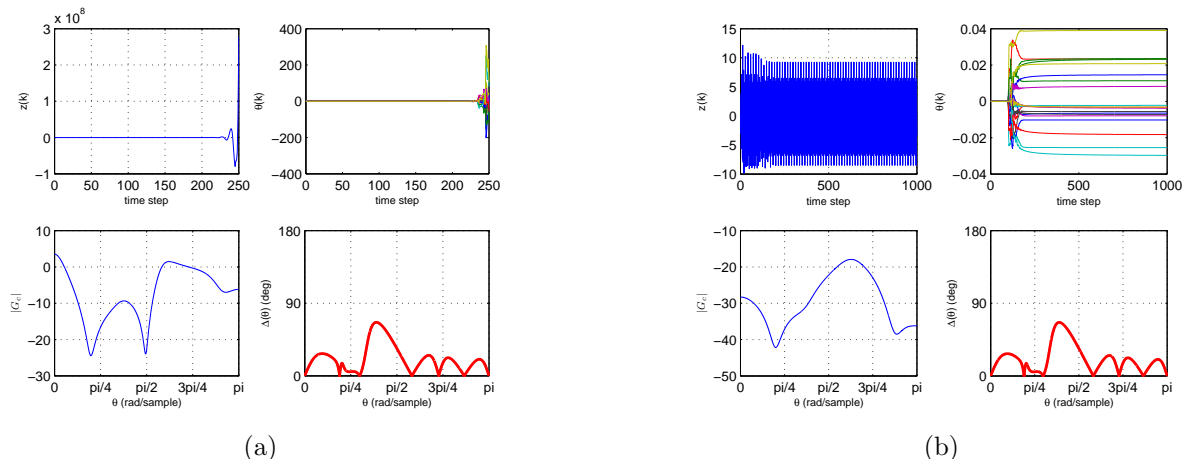


Figure 4. Example VI.2: SISO, NMP, asymptotically stable plant with the cumulative update law. The algorithm is modified to have a constant weighting term $\eta(k)$. (a) shows the closed-loop response with $\eta(k) \equiv 5$, where z diverges to infinity, while (b) shows the closed-loop response with $\eta(k) \equiv 10$, where z is not driven to zero.

Finally, if $\eta(k) \equiv 0$, the algorithm is similar to the cumulative RCAC algorithm described in [5]. In this case, we choose K_{zu} so that the NMP zeros of G_{zu} are a subset of the zeros of G_f . For instance, taking $K_{zu} = \begin{bmatrix} 1 & -3.25 & 2.5 \end{bmatrix}$, the zeros of G_f are 2 and 1.25, which are the NMP zeros of G_{zu} . Letting $n_c = 10$ and $P_0 = I$, the closed-loop response is shown in Figure 5. ■

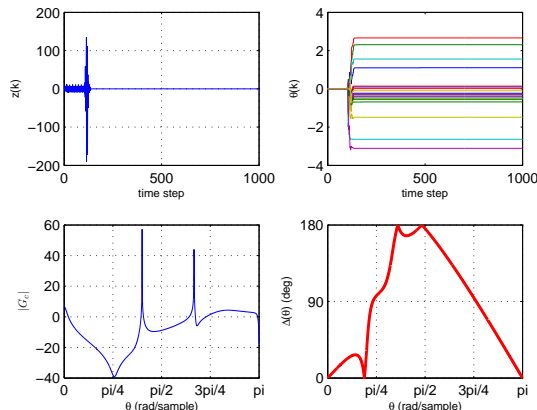


Figure 5. Example VI.2: SISO, NMP, asymptotically stable plant with the cumulative update law. This figure shows the closed-loop response with NMP-based K_{zu} construction, using the tuning parameters $n_c = 10$, $\eta_0 = 0.0$, and $P_0 = I$. The performance variable converges to zero. The transient peak is worse than the phase-matching-based results of Figure 3, however, the convergence is faster. These results suggest that smaller phase mismatch for $\theta \in [0, \pi]$ provides better transients.

Example VI.3 (2×2 , asymptotically stable plant with minimum-phase transmission zeros). Consider the stable, two-input, two-output plant

$$G_{zu}(z) = \begin{bmatrix} \frac{z-1.3}{(z-0.2+j0.6)(z-0.2-j0.6)} & \frac{2(z-0.3)}{(z-0.2+j0.6)(z-0.2-j0.6)} \\ \frac{z-0.2}{(z-0.2+j0.6)(z-0.2-j0.6)} & \frac{0.5(z-0.4)}{(z-0.2+j0.6)(z-0.2-j0.6)} \end{bmatrix} \quad (45)$$

with the transmission zeros 0.26 and 0.36. Although the channel $G_{zu,11}$ is nonminimum-phase, all of the transmission zeros of G_{zu} are minimum phase, therefore $K_{zu} = H_1$ suffices. With $G_{zu} \sim (A, B, E_1, 0)$ realized in the form

$$A = \begin{bmatrix} 0.4 & -0.8 & 0 & 0 \\ 0.5 & 0 & 0 & 0 \\ 0 & 0 & 0.4 & -0.8 \\ 0 & 0 & 0.5 & 0 \end{bmatrix}, \quad B = \begin{bmatrix} 2 & 0 \\ 0 & 0 \\ 0 & 2 \\ 0 & 0 \end{bmatrix}, \quad E_1 = \begin{bmatrix} 0.5 & -1.3 & 1.0 & -0.6 \\ 0.5 & -0.2 & 0.25 & -0.2 \end{bmatrix}, \quad (46)$$

we consider the command following and unmatched disturbance rejection problem with $D_1 = \begin{bmatrix} I_{3 \times 3} & 0_{3 \times 2} \\ 0_{1 \times 3} & 0_{1 \times 2} \end{bmatrix}$,

$E_0 = \begin{bmatrix} 0_{2 \times 3} & I_{2 \times 2} \end{bmatrix}$, and the exogenous signal $w(k) = \begin{bmatrix} w_1(k) & w_2(k) & w_3(k) & w_4(k) & w_5(k) \end{bmatrix}^T$, where $w_i(k) = \sin \theta_i k$ with $\theta_1 = 2\pi/13$ rad/sample, $\theta_2 = \pi/4$ rad/sample, $\theta_3 = 2\pi/5$ rad/sample, $\theta_4 = 2\pi/7$ rad/sample, and $\theta_5 = 2\pi/3$ rad/sample. We choose $n_c = 14$, $P_0 = I$, $\eta_0 = 0$, and $K_{zu} = H_1$. Figure 6 illustrates that the performance converges to zero. ■

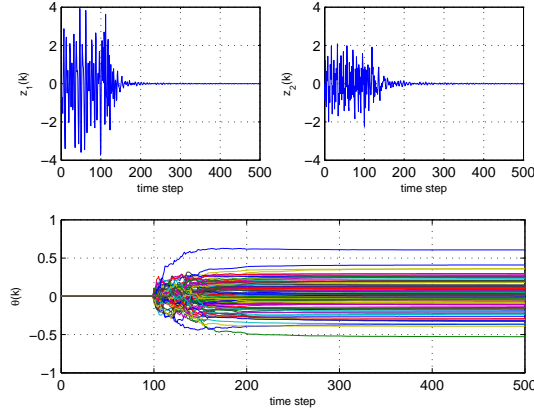


Figure 6. Example VI.3: 2×2 square, asymptotically stable plant with MP transmission zeros, and one NMP channel zero. The controller is turned on at $k = 100$. We choose $\eta_0 = 0$ and $K_{zu} = H_1$. The performance variables z_1 and z_2 converge to zero.

Example VI.4 (2×2 , asymptotically stable plant with nonminimum-phase transmission zeros). Consider the stable, two-input, two-output plant

$$G_{zu}(z) = \begin{bmatrix} \frac{-3(z-0.5+j0.3)(z-0.5-j0.3)}{\alpha(z)} & \frac{2(z-1.2)(z-1.5)}{\alpha(z)} \\ \frac{1.5(z-1.4+j0.7)(z-1.4-j0.7)}{\alpha(z)} & \frac{-0.5(z+1.1)(z-0.5)}{\alpha(z)} \end{bmatrix} \quad (47)$$

with $\alpha(z) = (z-0.4)(z-0.5-j0.5)(z-0.5+j0.5)$. Note that $G_{zu}(z)$ has minimum-phase transmission zero 0.923, and nonminimum-phase transmission zeros $0.907 \pm j0.648$, 7.86. We realize $G_{zu} \sim (A, B, E_1, 0)$ such that

$$A = \begin{bmatrix} 1.4 & -0.45 & 0.2 & 0 & 0 & 0 \\ 2 & 0 & 0 & 0 & 0 & 0 \\ 0 & 0.5 & 0 & 0 & 0 & 0 \\ 0 & 0 & 0 & 1.4 & -0.45 & 0.2 \\ 0 & 0 & 0 & 2 & 0 & 0 \\ 0 & 0 & 0 & 0 & 0.5 & 0 \end{bmatrix}, \quad B = \begin{bmatrix} 2 & 0 \\ 0 & 0 \\ 0 & 0 \\ 0 & 0 \\ 0 & 0 \\ 0 & 0 \end{bmatrix}, \quad E_1 = \begin{bmatrix} -1.5 & 0.75 & -0.51 & 1 & -1.35 & 1.8 \\ 0.75 & -1.05 & 1.8375 & -0.25 & -0.075 & 0.1375 \end{bmatrix}, \quad (48)$$

and consider the command following and unmatched disturbance rejection problem with $D_1 = \begin{bmatrix} I_{3 \times 3} & 0_{3 \times 2} \\ 0_{3 \times 3} & 0_{3 \times 2} \end{bmatrix}$,

$E_0 = \begin{bmatrix} 0_{2 \times 3} & -I_{2 \times 2} \end{bmatrix}$, and the exogenous signal $w(k) = \begin{bmatrix} w_1(k) & w_2(k) & w_3(k) & w_4(k) & \mathbf{1}(k) \end{bmatrix}^T$, where $w_i(k) = \sin \theta_i k$ with $\theta_1 = 2\pi/11$ rad/sample, $\theta_2 = 2\pi/8$ rad/sample, $\theta_3 = \pi/2$ rad/sample, and $\theta_4 = 2\pi/6$ rad/sample.

We first choose $n_c = 16$, $P_0 = I$, $\eta_0 = 0.1$, $p_c = 1$, and construct K_{zu} such that, for each input-output channel, the phase mismatch $\Delta_{ij}(\theta) < 90$ deg for all $\theta \in [0, \pi]$. In particular, we choose $K_{zu} = \begin{bmatrix} \kappa_1 & \kappa_2 & \kappa_3 & \kappa_4 \end{bmatrix}$, where $\kappa_1 = H_1$, $\kappa_2 = \begin{bmatrix} 0 & -2.4725 \\ -1.9927 & -0.9647 \end{bmatrix}$, $\kappa_3 = \begin{bmatrix} 0 & -1.0916 \\ -0.4711 & -0.4596 \end{bmatrix}$, and $\kappa_4 = \begin{bmatrix} 0 & 1.7922 \\ 1.4666 & 0 \end{bmatrix}$. Note that the only nonminimum-phase transmission zero of $G_f(z)$ is 6.854, and therefore K_{zu} does not capture the locations of the nonminimum-phase transmission zeros of G_{zu} . The closed-loop response is shown in Figure 7(a).

We now set $\eta_0 = 0$, keep $n_c = 16$, $P_0 = I$, and construct K_{zu} using the time-series coefficients, that is, $K_{zu} = \begin{bmatrix} \beta_1 & \beta_2 & \beta_3 \end{bmatrix}$. Hence, K_{zu} captures the locations of the nonminimum-phase transmission zeros of G_{zu} . The closed-loop response is shown in Figure 7(b).

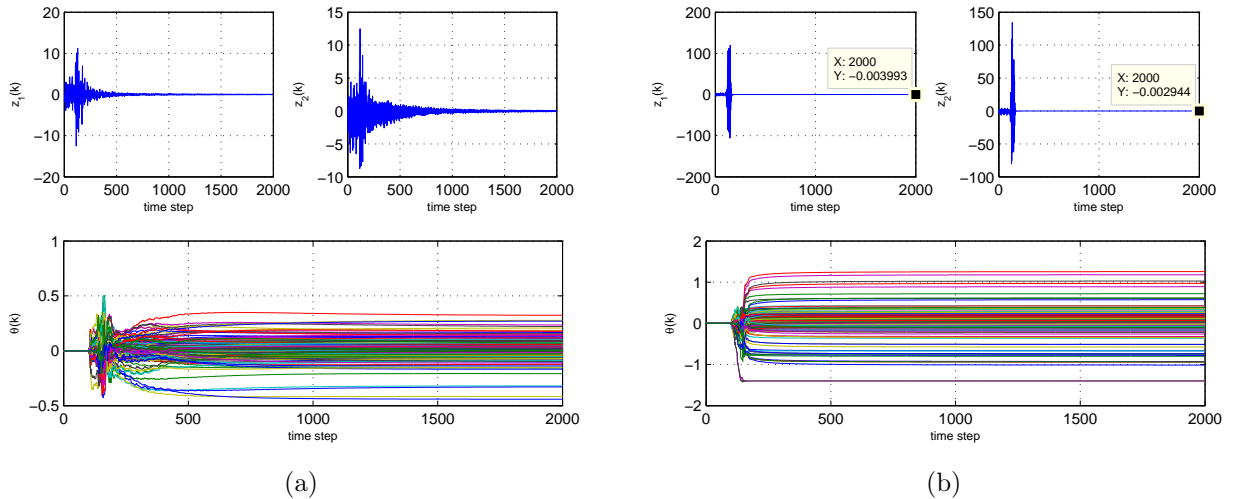


Figure 7. Example VI.4: 2×2 square, asymptotically stable plant with NMP transmission zeros, RCAC is turned on at $k = 100$. (a) shows the closed-loop response with phase-matching-based K_{zu} construction using $\eta_0 = 0.1$, while (b) shows the closed-loop response where K_{zu} is constructed using the time-series coefficients. In the latter case, K_{zu} captures the NMP transmission zeros of G_{zu} .

Finally, Figure 8 shows that the maximum value of the phase mismatch Δ_{ij} obtained in the first case where K_{zu} is constructed to bound Δ_{ij} by 40 deg, which is smaller than the maximum phase mismatch obtained in the case where K_{zu} is constructed using the time-series coefficients β_i for each channel. As in the SISO case, the results suggest that smaller channel-wise phase-mismatch leads to improved transient performance. ■

VII. Direction zeros in MISO and SIMO systems

Convergence of RCAC is shown in [3] for minimum-phase plants with the assumption that H_d is square and nonsingular.

In this section, we define the notion of a direction zero for two special non-square cases: Multiple-input, single-output (MISO) and single-input, multiple-output (SIMO) plants. Examples illustrating the effect of direction zeros in RCAC applications to MISO and SIMO plants are shown in Section VIII.

A. MISO Plants

In this section, we develop the notion of *input-direction zeros* in MISO plants, thus, $l_z = 1$, and $l_u > 1$. Throughout the discussion, we assume that all the entries $G_{zu,i}$ of the plant $G_{zu}(z) \in \mathbb{C}^{l_z \times l_u}$ are coprime fractions, and, for all $1 \leq i \leq l_u$, there exists $z_i \in \mathbb{C}$ such that $G_{zu,i}(z_i) \neq 0$. Furthermore, we assume that the triple (A, B, E_1) is a controllable and observable realization of G_{zu} , and let n denote the McMillan degree of G_{zu} . For $1 \leq i \leq n$, λ_i denote the eigenvalues of A .

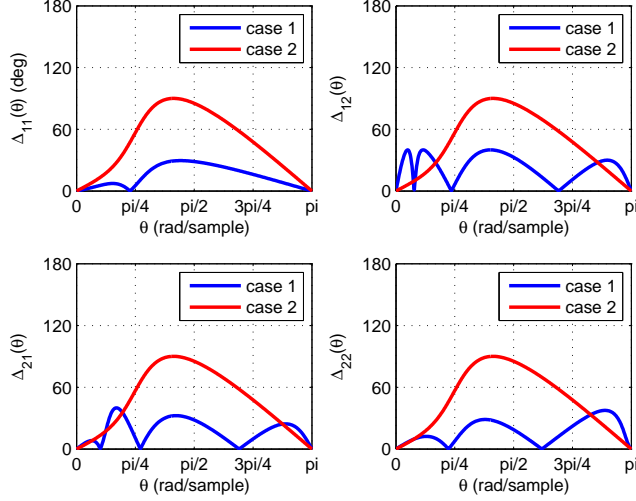


Figure 8. Example VI.4: Channel-wise phase mismatch functions $\Delta_{ij}(\theta)$ with phase-matching-based K_{zu} construction (case 1) and β_i -based construction (case 2). Note that Δ_{ij} in case 2 is the same for each channel. This is expected, since the numerator of $G_{f,ij}$ and $G_{zu,ij}$ is the same for each channel, the phase mismatch depends only on the denominator $\alpha(z)$, which is common for each channel.

Definition VII.1. Let $\mathcal{D} \neq 0 \in \mathbb{R}^{l_u}$, and $\zeta \neq \lambda_i \in \mathbb{C}$. Then, $\zeta \in \mathbb{C}$ is an input-direction zero of G_{zu} associated with the direction \mathcal{D} if

$$G_{zu}(\zeta)\mathcal{D} = 0. \quad (49)$$

According to Definition VII.1, ζ is assigned to a nonzero input direction \mathcal{D} , not vice-versa. Therefore, we use the terminology *direction zero*, instead of “zero direction”.

Proposition VII.2. $\zeta \neq \lambda_i$ is an input-direction zero of G_{zu} associated with \mathcal{D} if and only if there exists $x_0 \in \mathbb{C}^n$ such that

$$\Sigma(\zeta) \begin{bmatrix} x_0 \\ \mathcal{D} \end{bmatrix} = \begin{bmatrix} 0_{n \times 1} \\ 0 \end{bmatrix}, \quad (50)$$

where

$$\Sigma(z) \triangleq \begin{bmatrix} zI - A & B \\ E_1 & 0 \end{bmatrix} \in \mathbb{C}^{(n+1) \times (n+l_u)}. \quad (51)$$

Proof. We first show that if (50) holds for some x_0 , then $G_{zu}(\zeta)\mathcal{D} = 0$. Indeed,

$$\begin{bmatrix} \zeta I - A & B \\ E_1 & 0 \end{bmatrix} \begin{bmatrix} x_0 \\ \mathcal{D} \end{bmatrix} = \begin{bmatrix} 0_{n \times 1} \\ 0 \end{bmatrix} \Rightarrow \begin{bmatrix} (\zeta I - A)^{-1} & 0 \\ 0 & 1 \end{bmatrix} \begin{bmatrix} \zeta I - A & B \\ E_1 & 0 \end{bmatrix} \begin{bmatrix} x_0 \\ \mathcal{D} \end{bmatrix} = \begin{bmatrix} 0_{n \times 1} \\ 0 \end{bmatrix}, \quad (52)$$

$$\Rightarrow \begin{bmatrix} I & 0 \\ E_1 & -1 \end{bmatrix} \begin{bmatrix} I & (\zeta I - A)^{-1}B \\ E_1 & 0 \end{bmatrix} \begin{bmatrix} x_0 \\ \mathcal{D} \end{bmatrix} = \begin{bmatrix} 0_{n \times 1} \\ 0 \end{bmatrix}, \quad (53)$$

$$\Leftrightarrow \begin{bmatrix} I & (\zeta I - A)^{-1}B \\ 0 & G_{zu}(\zeta) \end{bmatrix} \begin{bmatrix} x_0 \\ \mathcal{D} \end{bmatrix} = \begin{bmatrix} 0_{n \times 1} \\ 0 \end{bmatrix}, \quad (54)$$

$$\Rightarrow G_{zu}(\zeta)\mathcal{D} = 0. \quad (55)$$

Next, we show the converse, that is, if $G_{zu}(\zeta)\mathcal{D} = 0$, then $\exists x_0 \in \mathbb{C}^n$ such that (50) holds. Let $x_0 = -(\zeta I - A)^{-1}B\mathcal{D}$. Then, (54) holds, therefore, (53) holds. Since

$$\text{rank} \begin{bmatrix} I & 0 \\ E_1 & -1 \end{bmatrix} = \text{rank} \begin{bmatrix} (\zeta I - A)^{-1} & 0 \\ 0 & 1 \end{bmatrix} = n + 1, \quad (56)$$

(53) gives (50). \square

Corollary VII.3. *An input-direction zero ζ of G_{zu} associated with an input direction \mathcal{D} is not necessarily a transmission zero of G_{zu} .*

Proof. Since $l_u > l_z = 1$, $\Sigma(z)$ has a nontrivial nullspace for all $z \in \mathbb{C}$. Therefore, $\Sigma(\zeta)$ may have full normal rank $n + 1$ while (50) is satisfied for some nonzero \mathcal{D} . In this case, ζ is an input-direction zero associated with \mathcal{D} , but not a transmission zero of G_{zu} .

Example VII.4. Consider the 1×2 SIMO plant $G_{zu}(z) = \begin{bmatrix} \frac{z-1.5}{(z-1.1)(z-0.4)} & \frac{z-0.5}{(z-1.1)(z-0.4)} \end{bmatrix}$. For $\mathcal{D} = \begin{bmatrix} 1 & 1 \end{bmatrix}^T$, $\zeta = 1$ satisfies (49), therefore, ζ is an input-direction zero associated with \mathcal{D} . Furthermore, G_{zu} has the state space realization

$$A = \begin{bmatrix} 0 & -0.44 \\ 1 & 1.5 \end{bmatrix}, \quad B = \begin{bmatrix} -0.75 & -0.25 \\ 0.5 & 0.5 \end{bmatrix}, \quad E_1 = \begin{bmatrix} 0 & 2 \end{bmatrix}, \quad E_2 = \begin{bmatrix} 0 & 0 \end{bmatrix}, \quad (57)$$

and

$$\Sigma(\zeta) = \begin{bmatrix} 1 & 0.44 & -0.75 & -0.25 \\ -1 & -0.5 & 0.5 & 0.5 \\ 0 & -2 & 0 & 0 \end{bmatrix}. \quad (58)$$

Note that, since $\Sigma(\zeta)$ has full normal rank, ζ is not a transmission zero of $(A, B, E_1, 0)$. Finally, it can be verified that $x_0 = \begin{bmatrix} 1 & 0 \end{bmatrix}$ is the unique solution of (50). \blacksquare

An input-direction zero associated with \mathcal{D} influences the input-output properties of a MISO system when the input sequence is linearly dependent with \mathcal{D} for all $k \geq 0$, that is, $u(k) = \mathcal{D}u_0(k)$, where $u_0(k)$ is a scalar. The following proposition demonstrates the *output-zeroing* [9, 10] effect of an input-direction zero.

Proposition VII.5. *For $\mathcal{D} \in \mathbb{R}^{l_u}$, let $\zeta \in \mathbb{C}$, $x_0 \in \mathbb{C}^n$ such that (50) holds. Then, the following statements hold.*

- (i) *For all $k \geq 0$, the state vector $x(k)$ and the output $z(k)$ with the initial condition $x(0) = -\text{Re}(x_0)$ and the input sequence $u(k) = \text{Re}(\zeta^k)\mathcal{D}$ satisfy*

$$x(k) = -\text{Re}(\zeta^k)\text{Re}(x_0) + \text{Im}(\zeta^k)\text{Im}(x_0), \quad (59)$$

$$z(k) = 0. \quad (60)$$

- (ii) *For all $k \geq 0$, the state vector $x(k)$ and the output $z(k)$ with the initial condition $x(0) = -\text{Im}(x_0)$ and the input sequence $u(k) = \text{Im}(\zeta^k)\mathcal{D}$ satisfy*

$$x(k) = -\text{Re}(\zeta^k)\text{Im}(x_0) + \text{Im}(\zeta^k)\text{Re}(x_0). \quad (61)$$

$$z(k) = 0, \quad (62)$$

Proof. Since the proofs are similar, we show only (i). For $k = 0$, (59) is obvious. Now, suppose (59) holds for some $k > 0$. We thus have

$$x(k+1) = Ax(k) + Bu(k) = -\text{Re}(\zeta^k)A\text{Re}(x_0) + \text{Im}(\zeta^k)A\text{Im}(x_0) + B\mathcal{D}\text{Re}(\zeta^k). \quad (63)$$

From (50), we have that

$$A\text{Im}(x_0) = \text{Re}(\zeta)\text{Im}(x_0) + \text{Im}(\zeta)\text{Re}(x_0), \quad (64)$$

$$B\mathcal{D} = A\text{Re}(x_0) - \text{Re}(\zeta)\text{Re}(x_0) + \text{Im}(\zeta)\text{Im}(x_0). \quad (65)$$

Substituting (64) and (65) into (63) yields

$$x(k+1) = (\text{Im}(\zeta^k)\text{Im}(\zeta) - \text{Re}(\zeta^k)\text{Re}(\zeta))\text{Re}(x_0) + (\text{Im}(\zeta^k)\text{Re}(\zeta) + \text{Im}(\zeta)\text{Re}(\zeta^k))\text{Im}(x_0) \quad (66)$$

$$= -\text{Re}(\zeta^{k+1})\text{Re}(x_0) + \text{Im}(\zeta^{k+1})\text{Im}(x_0). \quad (67)$$

Thus, if (59) holds for some k , it also holds for $k + 1$. By the principle of mathematical induction, we conclude that (59) holds for all $k \geq 0$. Finally, (50) implies that $E_1\text{Re}(x_0) = E_1\text{Im}(x_0) = 0$, hence, (60) follows. \square

Corollary VII.6. Let A be asymptotically stable, ζ be an input-direction zero of G_{zu} associated with \mathcal{D} and x_0 , and $u(k) = \text{Re}(\zeta^k)\mathcal{D}$ or $u(k) = \text{Im}(\zeta^k)\mathcal{D}$. Then, $z(k)$ exponentially converges to zero for all $x(0) \in \mathbb{R}^n$.

Proof. For $u(k) = \text{Re}(\zeta^k)$,

$$\begin{aligned} z(k) &= E_1 x(k) = E_1 A^k x(0) + \text{forced response} \\ &= E_1 A^k (x(0) + \text{Re}(x_0)) + E_1 A^k (-\text{Re}(x_0)) + \text{forced response}, \end{aligned}$$

thus, from Proposition VII.5, $z(k) = E_1 A^k (x(0) + \text{Re}(x_0))$. Since A is asymptotically stable, $z(k)$ exponentially converges to zero for all $x(0) \in \mathbb{R}^n$. The proof is similar for $u(k) = \text{Im}(\zeta^k)\mathcal{D}$.

Proposition VII.5 and Corollary VII.6 are demonstrated by the following examples respectively.

Example VII.7. Consider the 1×2 plant $G_{zu}(z) = \begin{bmatrix} \frac{z-1.5}{(z-1.1)(z-0.4)} & \frac{z-0.5}{(z-1.1)(z-0.4)} \end{bmatrix}$ with the state-space realization (57), and the input direction $\mathcal{D} = \begin{bmatrix} 1 & 1 \end{bmatrix}^T$. Note that the plant has an unstable pole 1.1. In Example VII.4, we have shown that $\zeta = 1$ is an input-direction zero associated with \mathcal{D} , and that $x_0 = \begin{bmatrix} 1 & 0 \end{bmatrix}^T$. We simulate G_{zu} with the initial condition $x(0) = -x_0$ and the input sequence $u(k) = \mathbf{1}(k)\mathcal{D}$. The trajectories of $x(k)$ and $z(k)$ are in accordance with (59), (60) as shown in Figure 9. ■

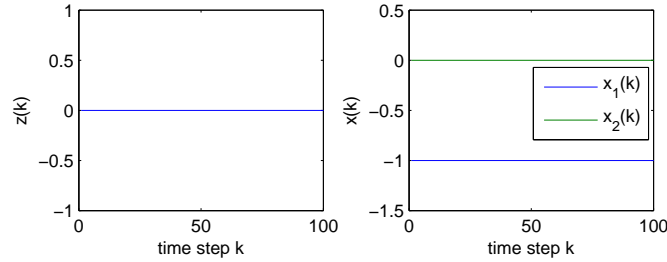


Figure 9. Example VII.7: For $\mathcal{D} = [1 \ 1]^T$, G_{zu} has the real input-direction zero $z_1 = 1$ and $x_0 = [1 \ 0]^T$. With $x(0) = -x_0$, exciting the plant with the input sequence $u(k) = \mathbf{1}(k)\mathcal{D}$ generates $z(k) = 0$, $x(k) = x(0)$, for $k \geq 0$.

Example VII.8. Consider the plant $G_{zu}(z) = \begin{bmatrix} 0.6z^2 - 0.1z + 0.21 & 0.2z^2 - 0.5z + 0.5 \end{bmatrix} / \alpha(z)$, where $\alpha(z) = (z - 0.9)(z - 0.4)(z - 0.3)$, and the input direction $\mathcal{D} = \begin{bmatrix} 1 & 2 \end{bmatrix}^T$. Solving (49), we have the input-direction zeros $z_{1,2} = 1.1e^{\pm j\pi/3}$ that are located outside the unit disk.

First, for $k \geq 0$, we simulate G_{zu} with zero initial condition $x(0) = 0$ and the input sequence $u(k) = \text{Re}\{1.1^k e^{j\pi k/3}\}\mathcal{D} = 1.1^k \cos(\pi k/3)\mathcal{D}$. Figure 10 shows that $z(k)$ converges to zero and the input $u(k)$ grows unboundedly as k increases. Similar results are obtained with the input sequence $u(k) = \text{Im}\{1.1^k e^{j\pi k/3}\}\mathcal{D} = 1.1^k \sin(\pi k/3)\mathcal{D}$ as shown in Figure 11. ■

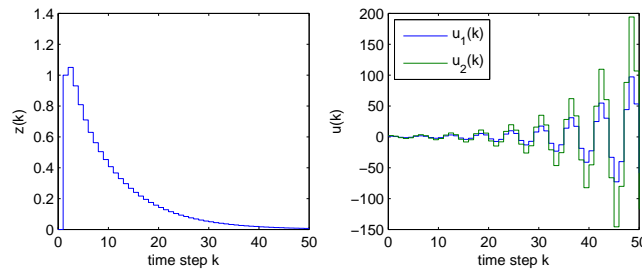


Figure 10. Example VII.8: For $\mathcal{D} = [1 \ 2]^T$, G_{zu} has complex input-direction zeros $z_{1,2} = 1.1e^{j\pi/3}$. With $x(0) = 0$ and the unbounded input sequence $u(k) = \text{Re}\{1.1^k e^{j\pi k/3}\}\mathcal{D} = 1.1^k \cos(\pi k/3)\mathcal{D}$, $z(k)$ converges to zero in accordance with Corollary VII.6.

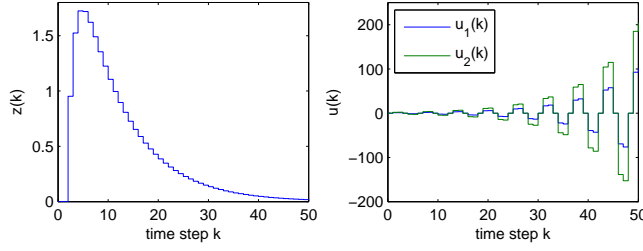


Figure 11. Example VII.8: For $\mathcal{D} = [1 \ 2]^T$, G_{zu} has complex input-direction zeros $z_{1,2} = 1.1e^{j\pi/3}$. With $x(0) = 0$ and the unbounded input sequence $u(k) = \text{Im}\{1.1^k e^{j\pi k/3}\}\mathcal{D} = 1.1^k \sin(\pi k/3)\mathcal{D}$, $z(k)$ converges to zero in accordance with Corollary VII.6.

B. SIMO Plants

We now develop the notion of *output-direction zeros* for SIMO plants, thus, $l_z > 1$, and $l_u = 1$. As in the MISO case, we assume that each entry of the plant $G_{zu}(z) \in \mathbb{C}^{l_z \times l_u}$ is a nonzero coprime fraction, the triple (A, B, E_1) is controllable and observable, and let n denote the McMillan degree of G_{zu} . For $1 \leq i \leq n$, λ_i denote the eigenvalues of A .

Definition VII.9. Let $\mathcal{D} \neq 0 \in \mathbb{R}^{1 \times l_z}$, and $\zeta \neq \lambda_i \in \mathbb{C}$. Then, $\zeta \in \mathbb{C}$ is an output-direction zero of $G_{zu}(z)$ corresponding to the output direction \mathcal{D} if

$$\mathcal{D}G_{zu}(\zeta) = 0. \quad (68)$$

Since $\mathcal{D} \in \mathbb{R}^{1 \times l_z}$ and $G_{zu} \in \mathbb{C}^{l_z \times 1}$, $\mathcal{D}G_{zu}(z)$ is a scalar function of z . In particular, $\mathcal{D}G_{zu}$ is a SISO plant whose output is $\mathcal{D}z(k)$, where $z(k)$ is the output of G_{zu} . Furthermore, $\mathcal{D}G_{zu}$ can be realized by the triplet $(A, B, \mathcal{D}E_1)$, which may not be minimal. However, we assume that the pair $(A, \mathcal{D}E_1)$ is observable. Thus, an output-direction zero ζ of G_{zu} associated with \mathcal{D} is a zero of the SISO plant $\mathcal{D}G_{zu}$, and, therefore, ζ satisfies

$$\begin{bmatrix} \zeta I - A & B \\ \mathcal{D}E_1 & 0 \end{bmatrix} \begin{bmatrix} x_0 \\ u_0 \end{bmatrix} = \begin{bmatrix} 0_{n \times 1} \\ 0 \end{bmatrix}, \quad (69)$$

where $x_0 \in \mathbb{C}^n$, $u_0 \in \mathbb{C}$. Note that since $(A, \mathcal{D}E_1)$ is observable, x_0 satisfying (69) cannot be an eigenvector of A . Consequently, u_0 cannot be equal to zero, because otherwise the upper equation in (69) would not hold. Now, since $u_0 \neq 0$, we can rewrite (69) as

$$\begin{bmatrix} \zeta I - A & B \\ \mathcal{D}E_1 & 0 \end{bmatrix} \begin{bmatrix} \bar{x}_0 \\ 1 \end{bmatrix} = \begin{bmatrix} 0_{n \times 1} \\ 0 \end{bmatrix}, \quad (70)$$

where $\bar{x}_0 = \frac{x_0}{u_0}$. The following proposition demonstrates the relationship between the output-direction zeros and the output $\mathcal{D}z(k)$ of the SISO plant $\mathcal{D}G_{zu}$.

Proposition VII.10. For $\mathcal{D} \in \mathbb{R}^{1 \times l_z}$, let $\zeta \in \mathbb{C}$, $\bar{x}_0 \in \mathbb{C}$ such that (70) holds. Then, the following hold

- (i) For all $k \geq 0$, the state vector $x(k)$ and the output $z(k)$ with the initial condition $x(0) = -\text{Re}(\bar{x}_0)$ and the input sequence $u(k) = \text{Re}(\zeta^k)$ satisfy

$$x(k) = -\text{Re}(\zeta^k)\text{Re}(\bar{x}_0) + \text{Im}(\zeta^k)\text{Im}(\bar{x}_0), \quad (71)$$

$$\mathcal{D}z(k) = 0. \quad (72)$$

- (ii) For all $k \geq 0$, the state vector $x(k)$ and the output $z(k)$ with the initial condition $x(0) = -\text{Im}(\bar{x}_0)$ and the input sequence $u(k) = \text{Im}(\zeta^k)$ satisfy

$$x(k) = -\text{Re}(\zeta^k)\text{Im}(\bar{x}_0) + \text{Im}(\zeta^k)\text{Re}(\bar{x}_0), \quad (73)$$

$$\mathcal{D}z(k) = 0. \quad (74)$$

Proof. The proof uses (70) and is similar to the proof of Proposition VII.5.

The above proposition indicates that, if G_{zu} has an output-direction zero ζ outside the unit disk or repeated on the unit circle, then the matrix multiplication $\mathcal{D}z(k)$ may be identically equal to zero for all k with an unbounded input signal, where \mathcal{D} is the associated output direction. In this case, if G_{zu} does not have a transmission zero at ζ , then $z(k)$ is unbounded. Furthermore, similar to Corollary VII.6, it can be shown that if A is asymptotically stable, then $\mathcal{D}z(k)$ exponentially converges to zero for all $x(0) \in \mathbb{R}^n$ with the input sequence $u(k) = \text{Re}(\zeta^k)$ or $u(k) = \text{Im}(\zeta^k)$.

VIII. Direction Zeros and RCAC

We now demonstrate the significance of direction zeros for adaptive control of MISO and SIMO systems using RCAC. The discussion is limited to MISO and SIMO systems. Furthermore, we consider only the case where K_{zu} is constructed using one coefficient, that is,

$$K_{zu} = \begin{bmatrix} 0_{l_z \times (r-1)l_u} & K_r \end{bmatrix}, \quad (75)$$

where r is a positive integer, and $K_r \neq 0 \in \mathbb{R}^{l_z \times l_u}$.

A. MISO Plants

In this section, we consider MISO plants, that is, $l_z = 1$, and $l_u \leq 2$.

1. Effect of the Input-Direction Zeros in the Control of MISO Systems with RCAC

First, we provide the following proposition that states that, for K_{zu} given as in (75), the direction of the input signal generated by RCAC is equal to K_r^T .

Proposition VIII.1. *For a positive integer r , let $K_{zu} = \begin{bmatrix} 0_{1 \times (r-1)l_u} & K_r \end{bmatrix}$, where $K_r \neq 0 \in \mathbb{R}^{1 \times l_u}$, and let the control $u(k)$ be generated by the control law (13) with either the instantaneous update law (26) or the cumulative update law (36)–(35) with $R_1(k) \equiv I$, $R_2(k) \equiv I$, $P(0) = \beta I$, $\beta > 0$, and $\Theta(0) = 0$. Then, $u(k)$ and K_r^T are linearly dependent for all $k \geq 1$, that is, $u(k) = K_r^T u_0(k)$, where $u_0(k)$ is a scalar.*

The proof of Proposition VIII.1 uses induction for both instantaneous and cumulative update laws. The implication of this proposition is as follows. Let G_{zu} be a MISO plant with no transmission zeros, and let us construct K_{zu} as shown in (75). Then, it follows from Proposition VIII.1 that the RCAC control input will have the form $u(k) = K_r^T u_0(k)$ and thus, the input-direction zeros of G_{zu} associated with K_r^T determines whether it is possible to have zero steady-state performance with an unbounded input sequence. In particular, it is shown in the numerical examples of Section 2 that if G_{zu} has NMP input-direction zeros associated with K_r^T , RCAC drives the performance to zero, but the control signal becomes unbounded at a rate determined by the magnitude of the NMP input-direction zeros, similar to the open-loop results demonstrated in Figures 10 and 11.

2. Numerical RCAC Examples Involving Input-Direction Zeros in MISO Plants

We now illustrate the effect of input-direction zeros in the control of MISO plants with RCAC. We use the cumulative cost with the recursive equations (34)–(36) with $\lambda = 1$. In all examples, we assume that the performance variable z is the only measurement and that $y = z$. Furthermore, in all cases, we initialize the controller gain vector $\Theta(0)$ and the controller states $x_c(0)$ to be zero.

Example VIII.2 (MISO, 1×4 , unstable plant, effect of input-direction zeros). Consider the unstable, 4 input, 1 output plant $G_{zu} = \begin{bmatrix} N_{11}(z) & N_{12}(z) & N_{13}(z) & N_{14}(z) \end{bmatrix} / \alpha(z)$, where $N_{11}(z) = 2.8(z-2)(z-1.4)(z-0.3)$, $N_{12}(z) = -2(z-0.1)(z-0.3+j0.3)(z-0.3-j0.3)$, $N_{13}(z) = 3(z+1.1)(z-0.2)(z-0.4)$, $N_{14}(z) = 0.5(z+1.03)(z+0.1)(z-0.6)$, and $\alpha(z) = (z-1.1)(z-0.05)(z-0.5+j0.5)(z-0.5-j0.5)$. We consider a combined disturbance rejection and command following problem with the disturbance $w_1(k) = \sin \frac{\pi}{7}k$, and the command $w_2(k) = \sin \frac{2\pi}{3}k + \sin \frac{\pi}{14}k$. We choose $K_{zu} = H_1$, $n_c = 10$, $\eta_0 = 0$, and $P_0 = I$. The plant G_{zu} has input-direction zeros $0.3063, 0.4911 \pm j0.818i$ associated with H_1 that are all located inside the unit

circle. Hence, RCAC drives the performance to zero, and the input vector remains bounded, as shown in Figure 12(a).

Now, we make a small modification so that G_{zu} has left H_1 -direction zeros of G_{zu} outside the unit circle. In particular, we let $N_{11}(z) = 3(z - 2)(z - 1.4)(z - 0.3)$, and keep other plant parameters the same. We consider the same command following and disturbance rejection problem, and choose $K_{zu} = H_1$, $n_c = 10$, $\eta_0 = 0$, and $P_0 = I$. With this choice, the modified plant has one left K_{zu} -direction zero 0.3055 inside the unit circle, and two left K_{zu} -direction zeros $0.5544 \pm j0.8374$ that are located outside the unit circle. Therefore the input vector diverges as shown in Figure 12(b). The performance variable z seems to converge to zero, but the simulation numerically crashes in about 2000 steps.

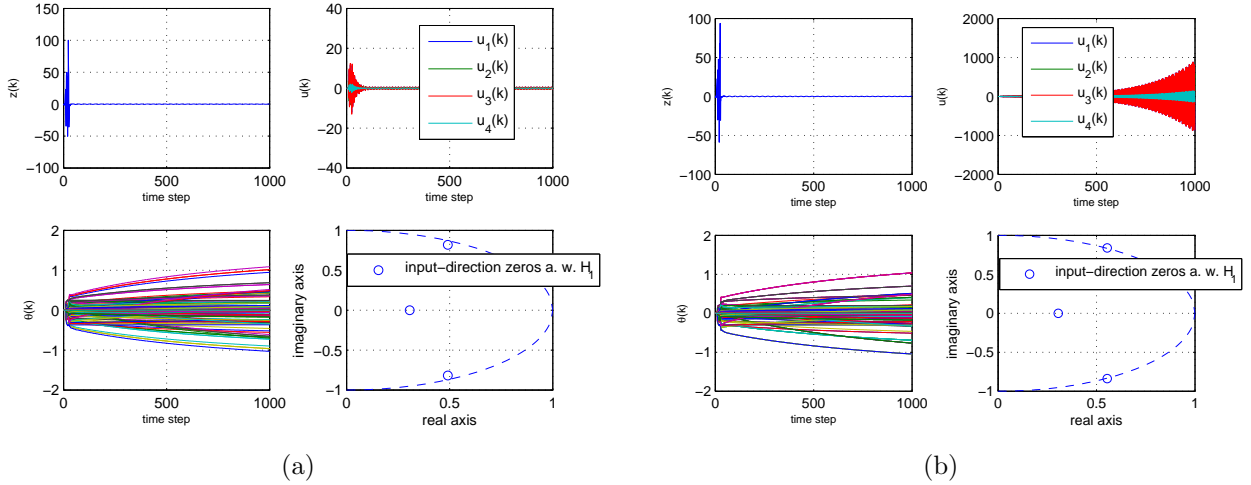


Figure 12. Example VIII.2: Unstable, MISO plant, command following and disturbance rejection with $K_{zu} = H_1$. (a) shows the closed-loop response of the original plant, whose input-direction zeros associated with H_1 are all located inside the unit circle, while (b) shows the closed-loop response of the modified plant, which has two input-direction zeros associated with H_1 outside the unit circle ($z_{1,2} = 0.5544 \pm j0.8374$). In the latter case, the input signal diverges due to the NMP input-direction zeros.

In the latter case, the plant was chosen so that the nonminimum-phase input-direction zeros are in the proximity of the unit circle, hence, the divergence of the input vector is slow. The divergence is faster when the nonminimum-phase input-direction zeros are located farther away from the unit circle. ■

B. SIMO Plants

In this section, we consider SIMO plants, that is, $l_u = 1$, and $l_z \leq 2$.

1. Effect of the Output-Direction Zeros in the Control of SIMO Systems with RCAC

We now consider the effects of the output-direction zeros in the control of SIMO systems when K_{zu} is constructed using one coefficient as in (75). Similar to the MISO case, if K_{zu} is constructed using one coefficient as in (75), the closed-loop performance of RCAC and the boundedness of the input signal is determined by the output-direction zeros associated with K_r^T . In particular, RCAC drives $K_r^T z(k)$ to zero, regardless of the location of the output-direction zeros. However, if G_{zu} has a NMP output-direction zero associated with K_r^T , then the control signal becomes unbounded, and the performance $z(k)$ grows unboundedly as well.

2. Numerical RCAC Examples Involving Output-Direction Zeros in SIMO Plants

We now illustrate the effect of output-direction zeros in the control of SIMO plants with RCAC. We use the cumulative cost with the recursive equations (34)–(36) with $\lambda = 1$. In all examples, we assume that the performance variable z is the only measurement and that $y = z$. Furthermore, in all cases, we initialize the controller gain vector $\Theta(0)$ and the controller states $x_c(0)$ to be zero.

Example VIII.3 (SIMO, 2×1 , asymptotically stable plant, effect of output-direction zeros). Consider the unstable, one input, two-output plant $G_{zu} = \frac{1}{\alpha(z)} \begin{bmatrix} N_{11}(z) & N_{21}(z) \end{bmatrix}^T$, where $N_{11}(z) = z - 1.2$, $N_{21}(z) = z - 0.7$, and $\alpha(z) = (z - 0.65 + j0.55)(z - 0.65 - j0.55)$. Note that this plant does not have any transmission zeros. We consider a matched disturbance rejection problem with the step disturbance $w(k) = \mathbf{1}(k)$. The tuning parameters $n_c = 5$, $\eta_0 = 0$, and $P_0 = I$ are fixed throughout the example.

We first choose $K_{zu} = K_1 = \begin{bmatrix} 1.3 & 1 \end{bmatrix}$. With this choice, G_{zu} has one right output-direction zero 0.9826 associated with K_1 that is located inside the unit circle. RCAC is turned on at $k = 500$, and drives the performance to zero as shown in Figure 13.

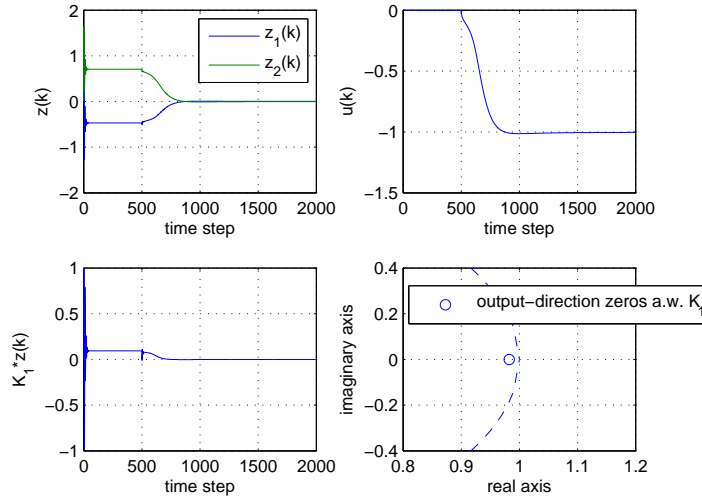


Figure 13. Example VIII.3: 2×1 SIMO plant, step disturbance rejection. We let $K_{zu} = K_1 = [1.3 \ 0]^T$, so that G_{zu} has the output-direction zero 0.9826 associated with K_1 . The performance $z(k)$ (and thus $K_1^T z(k)$) converges to zero, and the input vector remains bounded.

Now, we choose $K_{zu} = K_1 = \begin{bmatrix} 1.6 & 1 \end{bmatrix}$. With this choice, G_{zu} has the right output-direction zero 1.0077 associated with K_1 that is located outside the unit circle. RCAC is turned on at $k = 500$. The performance variable $z(k)$ diverges to infinity, although $K_1^T z(k)$ converges to zero. Furthermore, the input $u(k)$ diverges to infinity as shown in Figure 14 due to the NMP output-direction zero. ■

IX. Conclusions

In this paper, we extended the RCAC algorithm by removing the intermediate step of reconstructing the retrospective controls, and directly updating the controller. We extended the phase-matching condition to MIMO plants and presented a channel-wise controller construction method for MIMO, Lyapunov-stable plants with unknown nonminimum-phase zeros. We demonstrated the algorithm on several SISO and MIMO examples. We demonstrated the output-zeroing effect of left and right directions zero on MISO and SIMO plants. Numerical examples illustrated the effect of these direction zeros in MISO and SIMO RCAC applications, where the controller was constructed using one filter coefficient. Future work includes the investigation of direction zeros when the controller is constructed using multiple filter coefficients, and the analysis of direction zeros in MIMO non-square plants.

References

- ¹N. Hovakimyan, C. Cao, E. Kharisov, E. Xargay and I. M. Gregory, “ \mathcal{L}_1 Adaptive Control for Safety-Critical Systems,” *IEEE Control Systems Mag.*, vol. 31, no. 5, pp. 54–104, October 2011.
- ²R. Venugopal and D. S. Bernstein. “Adaptive Disturbance Rejection Using ARMARKOV System Representations,” *IEEE Trans. Contr. Sys. Tech.*, Vol. 8, pp. 257–269, 2000.
- ³J. B. Hoagg, M. A. Santillo, and D. S. Bernstein, “Discrete-Time Adaptive Command Following and Disturbance Rejection for Minimum Phase Systems with Unknown Exogenous Dynamics,” *IEEE Trans. Autom. Contr.*, Vol. 53, pp. 912–928, 2008.

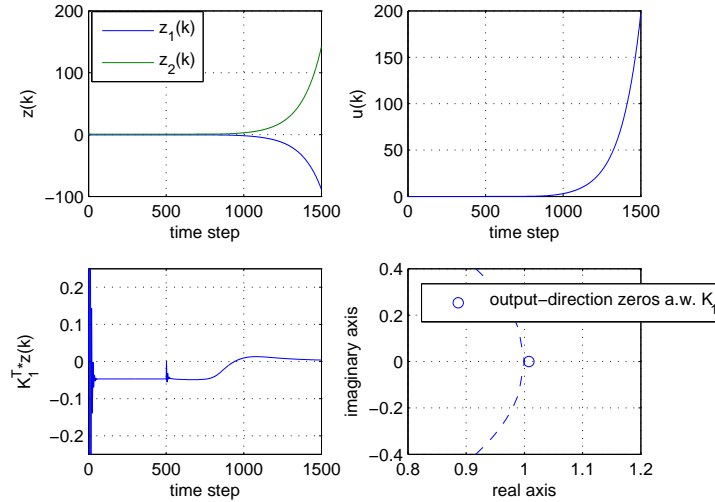


Figure 14. Example VIII.3: 2×1 SIMO plant, step disturbance rejection. We let $K_{zu} = K_1 = [1.6 \ 0]^T$, so that G_{zu} has the NMP output-direction zero 1.0077 associated with K_1 . The performance variable $z(k)$ and the input $u(k)$ diverge to infinity.

- ⁴M. A. Santillo and D. S. Bernstein, "Adaptive Control Based on Retrospective Cost Optimization," *AIAA J. Guid. Contr. Dyn.*, Vol. 33, pp. 289–304, 2010.
- ⁵J. B. Hoagg and D. S. Bernstein, "Retrospective Cost Adaptive Control for Nonminimum-Phase Discrete-Time Systems Part 1: The Ideal Controller and Error System; Part 2: The Adaptive Controller and Stability Analysis," *Proc. Conf. Dec. Contr.*, pp. 893–904, Atlanta, GA, December 2010.
- ⁶J. B. Hoagg and D. S. Bernstein, "Retrospective Cost Model Reference Adaptive Control for Nonminimum-Phase Discrete-Time Systems, Part 1: The Adaptive Controller; Part 2: Stability Analysis," *Proc. Amer. Contr. Conf.*, pp. 2927–2938, San Francisco, CA, June 2011.
- ⁷A. M. D'Amato, E. D. Sumer, and D. S. Bernstein, "Retrospective Cost Adaptive Control for Systems with Unknown Nonminimum-Phase Zeros," *AIAA Guid. Nav. Contr. Conf.*, Portland, OR, August 2011, AIAA-2011-6203.
- ⁸E. D. Sumer, A. M. D'Amato, A. M. Morozov, J. B. Hoagg, and D. S. Bernstein, "Robustness of Retrospective Cost Adaptive Control to Markov-Parameter Uncertainty," *Proc. Conf. Dec. Contr.*, pp. 6085–6090, Orlando, FL, December 2011.
- ⁹MacFarlane, A.G.J., and Karcanias, N., "Poles and Zeros of Linear Multivariable Systems: a Survey of the Algebraic, Geometric and Complex-Variable Theory," *Int. J. Contr.*, Vol. 24, No. 1, pp. 33-74, July 1976.
- ¹⁰J. Tokarzewski, "A General Solution to the Output-Zeroing Problem For MIMO LTI Systems," *Int. J. Appl. Math. Comput. Sci.*, vol. 12, no. 2, pp. 161–171, 2002.
- ¹¹J. B. Hoagg and D.S. Bernstein, "Cumulative Retrospective Cost Adaptive Control with RLS-Based Optimization," *Proc. Amer. Contr. Conf.*, Baltimore, MD, June 2010
- ¹²E. D. Sumer, M. H. Holzel, A. M. D'Amato, and D. S. Bernstein, "FIR-Based Phase Matching for Robust Retrospective-Cost Adaptive Control," *Proc. Amer. Conf. Contr.*, pp. 2707–2712, Montreal, Canada, June 2012.